ChemComm

Development of Catalytic Conversion of Nitrogen Molecule into Ammonia Using Molybdenum Complexes under Ambient Reaction Conditions

Journal:	*ChemComm*
Manuscript ID	CC-FEA-10-2020-007146.R1
Article Type:	Feature Article

FEATURE ARTICLE

Catalytic Conversion of Nitrogen Molecule into Ammonia Using Molybdenum Complexes under Ambient Reaction Conditions

Received 00th January 20xx,
Accepted 00th January 20xx

DOI: 10.1039/x0xx00000x

Yuya Ashida[a] and Yoshiaki Nishibayashi[a]

Nitrogen fixation using homogeneous transition metal complexes under mild reaction conditions is a challenging topic in the field of chemistry. Several successful examples of the catalytic conversion of nitrogen molecule into ammonia using various transition metal complexes in the presence of reductants and proton sources have been reported so far, together with detailed investigations on the reaction mechanism. Among those, only molybdenum complexes have been shown to serve as effective catalysts under ambient reaction conditions, in stark contrast with other transition metal-catalysed reactions that proceed at low reaction temperature such as –78 °C. In this feature article, we classify the molybdenum-catalysed reactions into four types: reactions via the Schrock cycle, reactions via dinuclear reaction systems, reactions via direct cleavage of the nitrogen–nitrogen triple bond of dinitrogen, and reactions via the Chatt-type cycle. We describe these catalytic systems focusing on the catalytic activity and mechanistic investigations. We hope that the present feature article provides useful information to develop more efficient nitrogen fixation systems under mild reaction conditions.

Introduction

Ammonia is one of the most important industrial chemicals. The amount of ammonia production reached 182 million metric tons in 2019, according to Mineral Commodity Summaries 2020.[1] About 75 to 90 percent of the ammonia produced in industry is converted to nitrogen-based fertilizers for worldwide food production.[2] Ammonia is also used as raw material for pharmaceuticals, plastics, textiles, explosives and other chemicals containing nitrogen atoms. Recently, ammonia has attracted attention not only as a raw material for fertilizers and chemicals but also as energy carrier.[3]

Today, ammonia is produced industrially by the Haber–Bosch process developed in the early 20th century.[4] In this process, ammonia is produced from the reaction of dinitrogen with dihydrogen using heterogeneous iron catalysts (Scheme 1a). This process is a powerful method that supports current chemical industry and food production. However, it requires high pressure (100–200 atm) and high temperature (300 °C–500 °C) to overcome the strong thermodynamic barrier (94.1 kJ/mol) for the dissociation of the nitrogen–nitrogen triple bond of the nitrogen molecule. In addition, dihydrogen as the raw material for ammonia production is obtained from fossil fuels.[4] The production of ammonia accounts for over 1.8% of the world's consumption of fossil fuels and ~1% of global carbon dioxide emissions (451 million metric tons per year).[2,3] Hence, the development of novel nitrogen fixation systems under mild and clean reaction conditions is highly desirable.

In nature, nitrogenase is a well-known enzyme that can fix dinitrogen and convert it into ammonia under ambient conditions (Scheme 1b).[5,6] The active site of nitrogenase has cluster structures containing transition metals (Mo, V or Fe), sulfur and carbon atoms. Nitrogenase

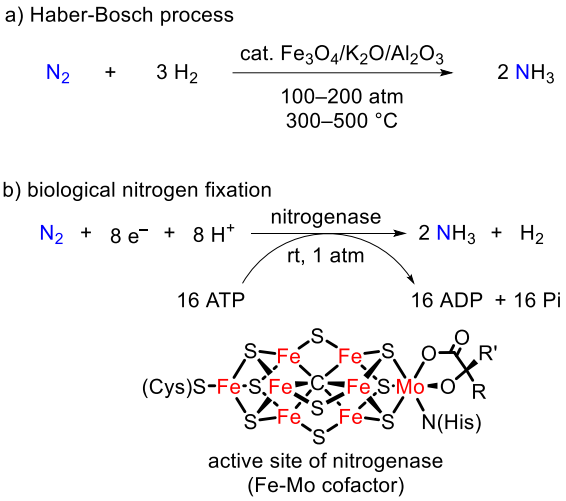

Scheme 1 Industrial and biological nitrogen fixation. (a) Typical Haber-Bosch process. (b) Biological ammonia formation with nitrogenase.

is classified into three groups depending on the transition metals. Among them, the enzyme containing molybdenum is known to be the most effective for nitrogen fixation. Reduction of dinitrogen by nitrogenase proceeds under ambient reaction conditions, where electrons, protons and adenosine triphosphate are consumed to produce ammonia, dihydrogen, adenosine diphosphate and phosphoric acids. The reaction rate of the formation of ammonia using nitrogenase (Fe–Mo cofactor) has been estimated to be up to 155 nmol ammonia per nmol Fe–Mo cofactor per min (TOF: up to 155 equiv/Mo min^{-1}) under various reaction conditions using $Na_2S_2O_4$ as a reductant.[7] On the basis of the structure of nitrogenase enzymes and their catalytic activity, the development of novel nitrogen fixation

[a] Department of Applied Chemistry, School of Engineering, The University of Tokyo, Hongo, Bunkyo-ku, Tokyo 113-8656, Japan. E-mail: ynishiba@sys.t.u-tokyo.ac.jp.

systems using homogeneous transition metal complexes as catalysts by mimicking the active site of nitrogenase has been envisaged.

In the last decades, various stoichiometric and catalytic conversion reactions of dinitrogen into ammonia have been reported.[8,9] Although a variety of homogeneous transition metal complexes (titanium,[10] vanadium,[11,12] iron,[13,14,15] cobalt,[16,17] molybdenum,[18,19,20] ruthenium[21] and osmium[21]) have been discovered as catalysts, only molybdenum complexes are effective under ambient reaction conditions. This feature article overviews the development of the conversion of nitrogen molecule into ammonia using molybdenum complexes, with a special focus on the reaction mechanism.

Stoichiometric Reactions

The first example of the formation of ammonia from coordinated dinitrogen was reported by Chatt and co-workers in 1975 (Scheme 2).[22] The reactions of *cis*-$[M(N_2)_2(PMe_2Ph)_4]$ or *trans*-$[M(N_2)_2(PMePh_2)_4]$ (M = Mo or W) with excess amount of sulfuric acid in MeOH at room temperature gave up to 0.66 and 1.98 equivalents of ammonia per molybdenum atom and per tungsten atom, respectively. In these reactions, the six electrons used for the formation of two ammonia molecules are supplied from the metal centre, which is oxidized from the oxidation state 0 to VI.

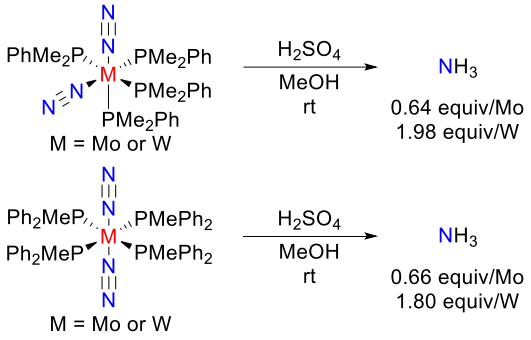

Scheme 2 Stoichiometric ammonia formation from molybdenum- and tungsten-dinitrogen complexes.

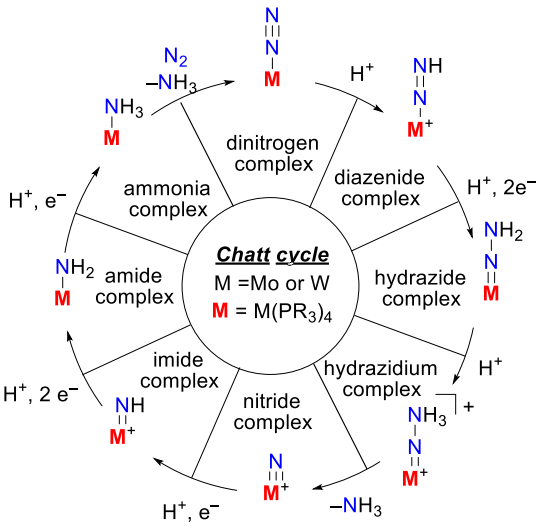

Scheme 3 Chatt cycle: virtual catalytic cycle using molybdenum- and tungsten-dinitrogen complexes.

After the report by Chatt, several research groups explored stoichiometric reactions of various metal dinitrogen complexes or other precursors to isolate related complexes such as diazenide (M–N=NH), hydrazide (M=N–NH_2), hydrazidium (M≡N–NH_3), nitride (M≡N), imide (M=NH) and amide (M–NH_2) complexes as key reactive intermediates.[23] From these results, 'the Chatt cycle' shown in Scheme 3 was proposed, in which dinitrogen is converted to ammonia via transition metal complexes containing zerovalent to tetravalent metal centres.[23] However, no successful example of the catalytic reaction following the Chatt cycle was reported until our recent findings.[9]

Schrock Cycle

The first successful example of the catalytic transformation of dinitrogen into ammonia under ambient reaction conditions using homogeneous transition metal complexes as catalysts was reported by Yandulov and Schrock in 2003.[18a] The reaction of an atmospheric pressure of dinitrogen with decamethylchromocene ($CrCp^*_2$, Cp^* = η^5-C_5Me_5) as a reductant and 2,6-lutidinium tetraarylborate ([LutH]BAr^F_4, Lut = 2,6-dimethylpyridine, Ar^F = 3,5-bis(trifluoromethyl)phenyl) as a proton source in the presence of a catalytic amount of a molybdenum dinitrogen complex bearing a triamidoamine ligand, i.e., $[Mo(N_2)(HIPTN_3N)]$ ($HIPTN_3N$ = (3,5-(2,4,6-*i*-$Pr_3C_6H_2)_2C_6H_3NCH_2CH_2)_3N$), in heptane at room temperature afforded 7.6 equivalents of ammonia per molybdenum atom (Scheme 4). Some reactive intermediates such as anionic dinitrogen ($[Mo(N_2)(HIPTN_3N)]^-$), diazenide ($[Mo(NNH)(HIPTN_3N)]$), hydrazide ($[Mo(NNH_2)(HIPTN_3N)]^+$), nitride ($[Mo(N)(HIPTN_3N)]$), imide ($[Mo(NH)(HIPTN_3N)]^+$) and ammonia complexes ($[Mo(NH_3)(HIPTN_3N)]^+$ and $[Mo(NH_3)(HIPTN_3N)]$) were prepared from protonation and/or reduction of the starting dinitrogen complex $[Mo(N_2)(HIPTN_3N)]$ and its derivatives.[24,25] On the basis of these experimental results, a plausible reaction pathway called the Schrock cycle, which includes trivalent to hexavalent molybdenum complexes as intermediates, was proposed by Schrock and co-workers (Scheme 5).[24] First, two reaction pathways can be considered for the conversion of $[Mo(N_2)(HIPTN_3N)]$ into the diazenide complex. One reaction pathway proceeds via stepwise reduction and protonation of the dinitrogen ligand through the formation of the corresponding anionic dinitrogen complex. The other reaction pathway involves conversion of the cationic dinitrogen complex resulting from the protonation of

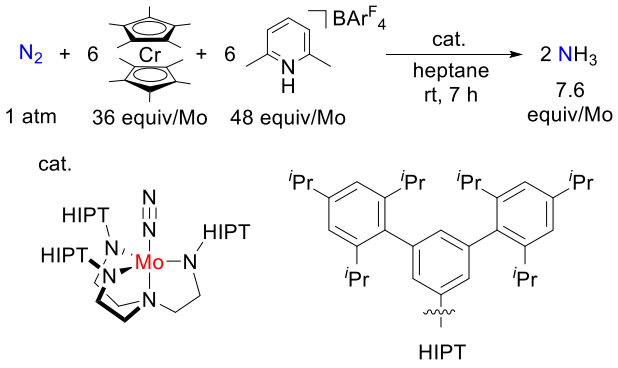

Scheme 4 Catalytic ammonia formation under ambient reaction conditions using molybdenum-dinitrogen complex bearing a triamideamine ligand.

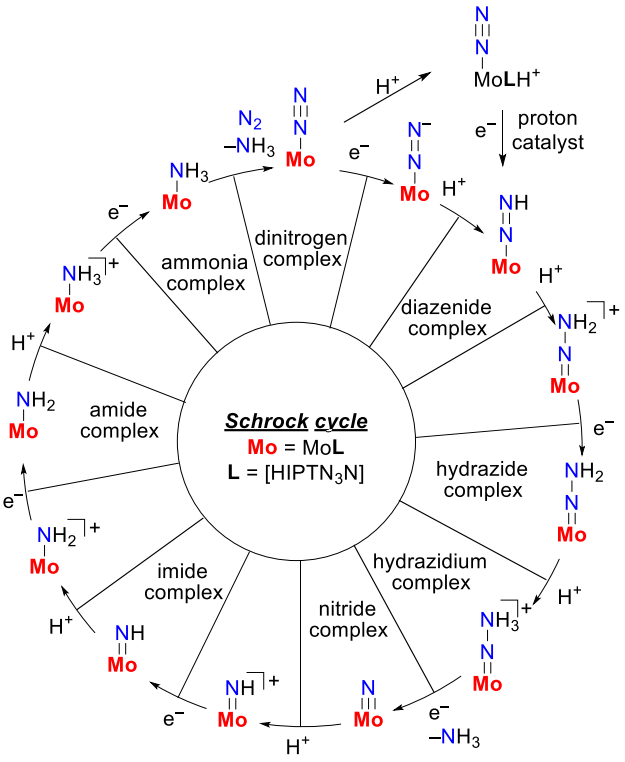

Scheme 5 Schrock cycle: plausible catalytic cycle using molybdenum-dinitrogen complex reported by Schrock and Yandulov.

the nitrogen atom of the amide group in [Mo(N$_2$)(HIPTN$_3$N)] into the corresponding diazenide complex via reduction and proton-catalysed isomerization. Next, in both cases, stepwise protonation and reduction of the diazenide complex proceeds to release one ammonia molecule and the corresponding nitride complex via hydrazide and hydrazidium complexes. Then, the nitride complex is converted to the ammonia complex through imide and amide complexes via alternation of protonation and reduction steps three times. Finally, an exchange of the ammonia ligand with another dinitrogen molecule occurs with the concomitant release of the second ammonia molecule, and [Mo(N$_2$)(HIPTN$_3$N)] is regenerated. In this catalytic cycle, some reactive intermediates such as [Mo(NNH)(HIPTN$_3$N)], [Mo(N)(HIPTN$_3$N)] and [Mo(NH$_3$)(HIPTN$_3$N)](BAr$^F_4$) were reported to show almost the same catalytic activity as the dinitrogen complex [Mo(N$_2$)(HIPTN$_3$N)].[18a]

Catalytic Cycle via Dinuclear Complexes

Our group reported the second successful example of catalytic ammonia formation under ambient reaction conditions in 2010, using a dinitrogen-bridged dimolybdenum complex bearing PNP-type pincer ligands, namely, [{Mo(N$_2$)$_2$(PNP)}$_2$(μ-N$_2$)] (PNP = 2,6-bis(di-*tert*-butylphosphinomethyl)pyridine), as a catalyst (Scheme 6).[19a] In the presence of a catalytic amount of [{Mo(N$_2$)$_2$(PNP)}$_2$(μ-N$_2$)], the reaction of an atmospheric pressure of dinitrogen with 108 equivalents of cobaltocene (CoCp$_2$, Cp = η^5-C$_5$H$_5$) per molybdenum atom as a reductant and 144 equivalents of 2,6-lutidinium triflate ([LutH]OTf, OTf = OSO$_2$CF$_3$) per molybdenum atom as a proton source in toluene at room temperature afforded 11.6 equivalents of ammonia per molybdenum atom, together with 21.7 equivalents of dihydrogen as a byproduct.

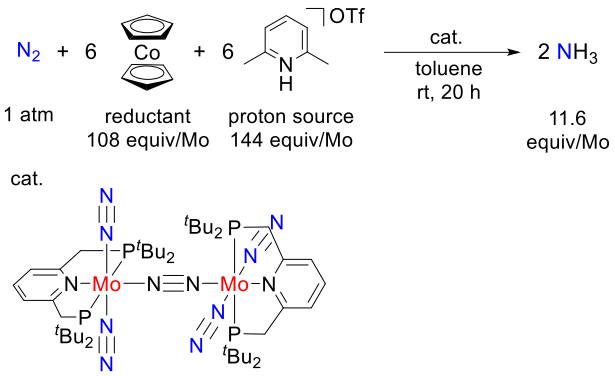

Scheme 6 Catalytic ammonia formation under ambient reaction conditions using dinitrogen-bridged dimolybdenum complex bearing PNP-type pincer ligands.

To obtain mechanistic information, some stoichiometric reactions were performed (Scheme 7).[19a,26] The reaction of [{Mo(N$_2$)$_2$(PNP)}$_2$(μ-N$_2$)] with 2 equivalents of HBF$_4$·OEt$_2$ and pyridine gave a hydrazide(2–) complex, i.e., ([Mo(F)(Py)(NNH$_2$)(PNP)](BF$_4$)) (Scheme 7a). However, unfortunately, the latter complex exhibited no catalytic activity under the same reaction conditions because the strong bond energy between the molybdenum and fluorine atoms inhibits the regeneration of the dinitrogen complex. The corresponding mononuclear nitride and imide complexes were separately isolated as plausible reactive intermediates (Scheme 7b). Fortunately, the nitride complexes [Mo(N)Cl(PNP)] and [Mo(N)Cl(PNP)][OTf] acted as effective catalysts, whereas nitride ([Mo(N)Cl$_2$(PCP)] and imide ([Mo(NH)Cl(Py)(PNP)] complexes did not. These results indicate that the strong coordination of chloride and pyridine ligands may prevent the regeneration of the dinitrogen complex. It was confirmed that the nitride ligand of [Mo(N)Cl(PNP)] can be converted into ammonia quantitatively under the catalytic reaction conditions (Scheme 7b).

To elucidate the mechanism of the reaction in which [{Mo(N$_2$)$_2$(PNP)}$_2$(μ-N$_2$)] acts as a catalyst, DFT calculations were independently conducted by Batista's group[27] and our groups,[26,28] although Batista's group did not estimate the activation energy in all steps. Both calculations revealed that the dinuclear structure plays important roles during the catalytic reaction. The reaction pathway proposed by our groups is shown in Scheme 8, which includes the free energy changes at 298 K and free energies of activation in the individual steps. According to these calculations, the dinuclear structure of [{Mo(N$_2$)$_2$(PNP)}$_2$(μ-N$_2$)] remains unaltered during the catalytic cycle. First, the formation of diazenide complex **I** from [{Mo(N$_2$)$_2$(PNP)}$_2$(μ-N$_2$)] proceeds via protonation and subsequent exchange of the terminal dinitrogen located at the *trans*-position of the diazenide ligand with the triflate anion derived from [LutH]OTf. Then, alternating protonation and reduction of **I** affords the corresponding nitride complex **II** with the concomitant release of one ammonia molecule. Subsequent alternating protonation and reduction steps from **II** gives ammonia complex **III**. Then, elimination of the ammonia ligand and coordination of a dinitrogen ligand occurs to give

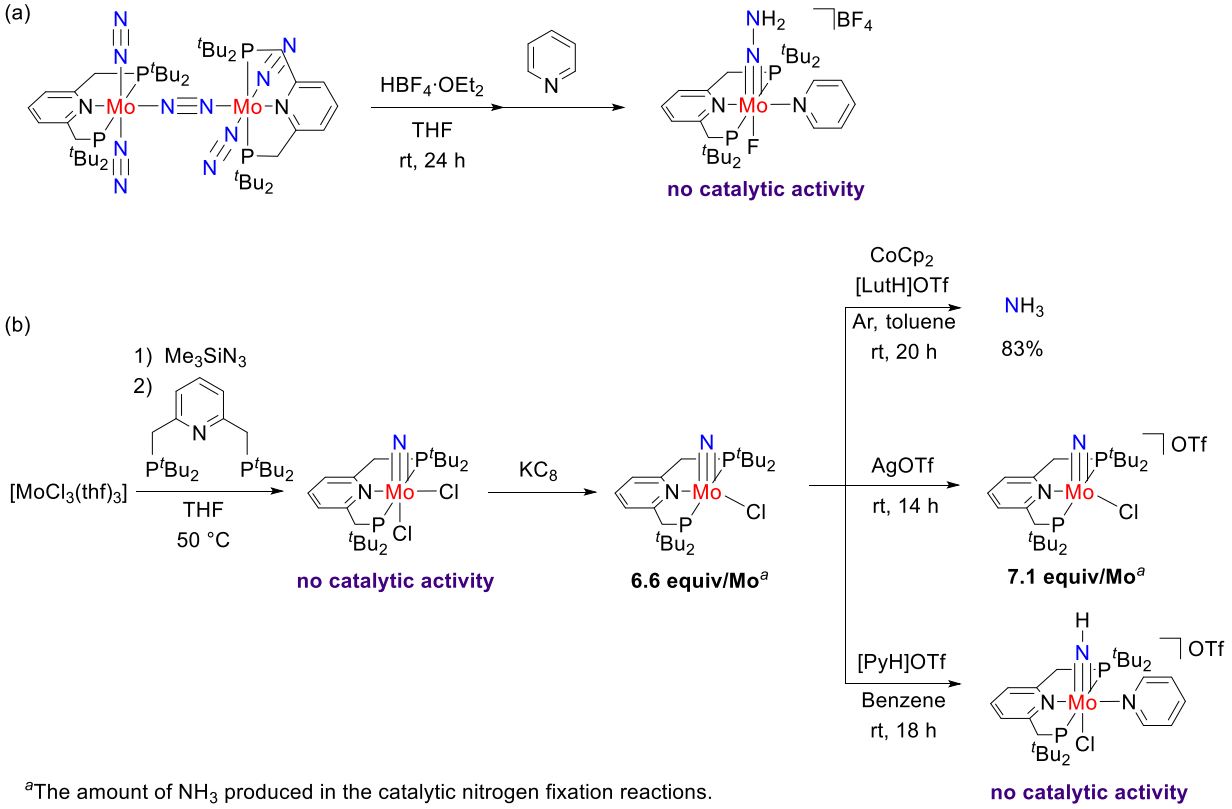

[a]The amount of NH_3 produced in the catalytic nitrogen fixation reactions.

Scheme 7 Stoichiometric reactions of molybdenum complexes bearing PNP-type pincer ligand.

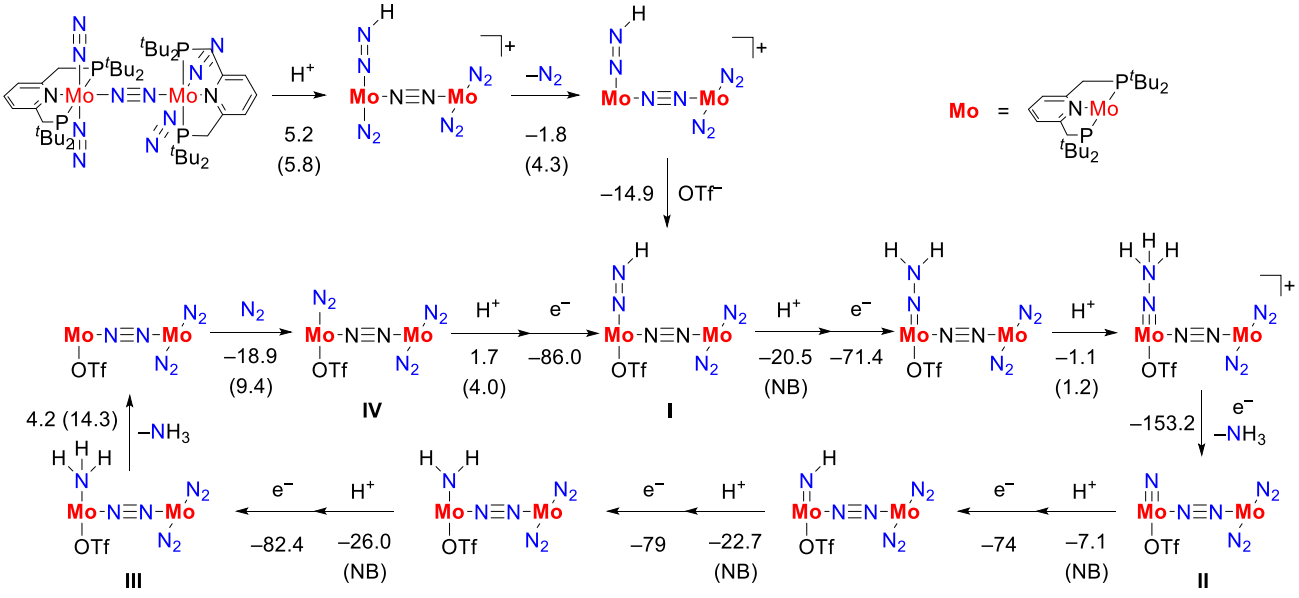

Free energy changes at 298 K and free energies of activation (in parenthesis) for individual steps were calculated at the B3LYP-D3 level of theory (units in kcal/mol). NB represents that the corresponding reaction has no activation barrier.

Scheme 8 Plausible reaction pathway using dinitrogen-bridged dimolybdenum complex bearing PNP-type pincer ligands.

dinitrogen complex **IV**. Finally, stepwise protonation and reduction of **IV** regenerates **I**. In this catalytic cycle, the first protonation of the coordinated dinitrogen ligand is the most endergonic process; therefore, facilitating the protonation step is important to improve the catalytic activity.

Our groups investigated the effect of substituents at the 4-position of the pyridine ring of the PNP ligand on the reduction of dinitrogen into ammonia catalysed by dinitrogen-bridged dimolybdenum complexes (Scheme 9).[29] The introduction of electron-donating substituents such as *tert*-butyl, methyl and methoxy groups increased the catalytic activity for ammonia formation,[29a] most likely due to the acceleration of the protonation steps by increased π-back donation and activation of the terminal dinitrogen ligand, as was suggested by infrared (IR) spectroscopy analysis and DFT calculations. On the other hand, no

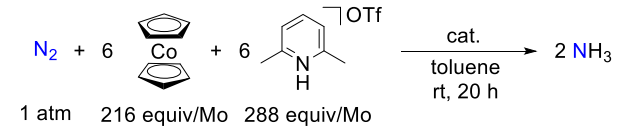

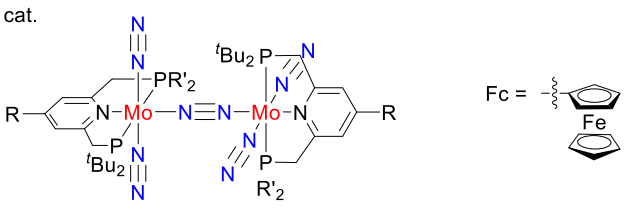

R	R'	NH_3 (equiv/Mo)	ν_{NN} (termical) (THF, cm^{-1})	ν_{NN} (termical) (KBr, cm^{-1})
H	^{t}Bu	12	1944	1936
Ph	^{t}Bu	10	1950	
Me_3Si	^{t}Bu	11	1947	
^{t}Bu	^{t}Bu	14	1939	
Me	^{t}Bu	15	1939	
MeO	^{t}Bu	17	1932	
Fc	^{t}Bu	18	1944	
H	Ad	9		1957
H	Ph	1[a]		1939

[a]72 equivalents of $CoCp_2$ and 96 equivalents of [Lut]OTf were used.

Scheme 9 Catalytic ammonia formation using various dinitrogen-bridged dimolybdenum complexes.

influence on the activation of the dinitrogen ligand was observed when introducing a ferrocenyl (Fc) group as a redox active moiety at the 4-position of the pyridine ring of the PNP ligand.[29b] However, the complex containing a Fc group showed higher catalytic activity than [{Mo(N2)2(PNP)}2(μ-N2)]. It was proposed that the electronic interaction between the molybdenum atom of the catalyst and the iron atom of the ferrocene moiety might accelerate the reduction step in the catalytic cycle.

Dinitrogen-bridged dimolybdenum complexes bearing PNP ligands with 1-adamantyl (Ad) or phenyl groups instead of *tert*-butyl groups on one of the phosphorus atoms of [{Mo(N2)2(PNP)}2(μ-N2)] were designed and prepared for comparison (Scheme 9).[30] The catalytic activity of these complexes for ammonia formation was investigated under similar reaction conditions as those for [{Mo(N2)2(PNP)}2(μ-N2)]. As a result, the introduction of phenyl groups on the phosphorus atoms decreased the amount of ammonia, and the complex containing 1-adamantyl groups exhibited similar catalytic activity to that of [{Mo(N2)2(PNP)}2(μ-N2)]. These results indicate that the presence of bulky substituents on the phosphorus atoms in the PNP ligand is an essential factor to promote the catalytic formation of ammonia from dinitrogen.

The use of a PPP-type pincer ligand (PPP = bis(di-*tert*-butylphosphinoethyl)phenylphosphine) in place of the PNP-type pincer ligand was investigated by our groups in 2015 (Scheme 10).[31] Since the PPP-type pincer ligand has weaker Brønsted basicity than the PNP-type pincer ligand, it is expected that the dissociation of the ligand from the metal centre caused by protonation of the ligand is prevented during the catalytic reaction. In the presence of a catalytic amount of [MoCl(N)(PPP)][BAr^F_4] or [MoCl(N)(PPP)], the reaction of an atmospheric pressure of dinitrogen with 36 equivalents of $CoCp^*_2$ and 48 equivalents of 2,4,6-colidinium triflate ([Col]OTf, Col = 2,4,6-trimethylpyridine) per molybdenum atom in toluene at room temperature afforded 9.3 or 11.0 equivalents of ammonia per molybdenum atom, respectively. The use of larger amounts of reductant and proton source in the presence of [MoCl(N)(PPP)][BAr^F_4] gave 63 equivalents of ammonia per molybdenum atom. Although the corresponding dinitrogen bridged complex was not isolated, reduction of [$MoCl_3$(PPP)] with reductants such as Na–Hg, KC_8 and $CoCp^*_2$ gave a mixture with a strong IR absorption derived from the terminal dinitrogen ligands (ν_{NN}(terminal) = 1944 cm^{-1} in THF). DFT calculations revealed the possibility of the formation of dinitrogen-bridged complex [{Mo(N2)2(PPP)}2(μ-N2)] with a similar structure to that of [{Mo(N2)2(PNP)}2(μ-N2)]. According to these results, the catalytic reaction was proposed to proceed via [{Mo(N2)2(PPP)}2(μ-N2)] as a key reactive intermediate.

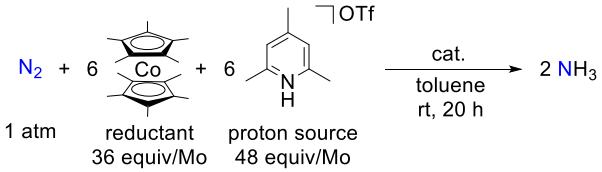

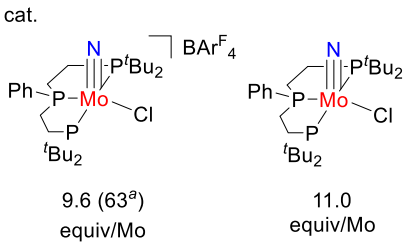

[a]540 equivalents of $CoCp^*_2$ and 720 equivalents of [Col]OTf were used.

Scheme 10 Catalytic ammonia formation using molybdenum-nitride complexes bearing triphosphine ligand.

A dinitrogen-bridged dimolybdenum complex bearing PCP-type pincer ligands [{Mo(N2)2(PCP)}2(μ-N2)] (PCP = 1,3-bis(di-*tert*-butylphosphinomethyl)benzimidazole-2-ylidene) proved to be an excellent catalyst (Scheme 11).[19b] The PCP ligand is characterized by its *N*-heterocyclic carbene moiety, which is known to coordinate more strongly than the pyridine moiety of the PNP ligand due to its high σ-donation ability. The reaction of an atmospheric pressure of dinitrogen with 720 equivalents of $CoCp^*_2$ and 960 equivalents of [LutH]OTf per molybdenum atom in the presence of a catalytic amount of [{Mo(N2)2(PCP)}2(μ-N2)] in toluene at room temperature for 20 hours afforded 100 equivalents of ammonia per molybdenum atom. The introduction of two methyl groups at the 5- and 6-positions of the benzimidazole ring of the PCP ligand as electron-donating groups increased the catalytic activity. A similar reaction pathway to that of [{Mo(N2)2(PNP)}2(μ-N2)] (Scheme 8) was proposed for this reaction.[26,28] Detailed experimental studies on the stability of [{Mo(N2)2(PCP)}2(μ-N2)] indicate that the dissociation of the PCP ligand was suppressed. Meanwhile, a dinitrogen-bridged dimolybdenum complex [{Mo(N2)2(PCP')}2(μ-N2)] (PCP': 1,3-bis(2-(di-*tert*-butylphosphino)ethyl)imidazole-2-ylidene) bearing similar

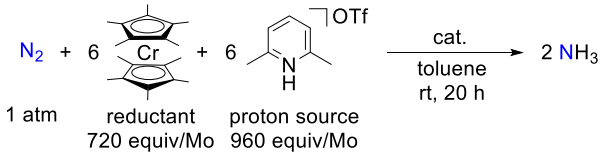

cat.		NH_3 (equiv/Mo)
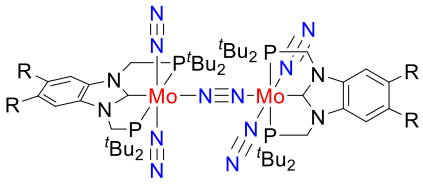	R = H	100
	R = Me	115
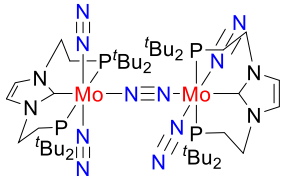		1.6[a]

[a]72 equivalents of $CrCp^*_2$ and 96 equivalents of [Lut]OTf were used.

Scheme 11 Catalytic ammonia formation using dinitrogen-bridged dimolybdenum complexes bearing PCP-type pincer ligands.

PCP-type pincer ligands with longer linkers between the NHC skeleton and the phosphorus atom did not catalyse the reaction. This lack of catalytic activity is due to the thermodynamic instability of the dinitrogen-bridged dimolybdenum structure in solution.

Catalytic Cycle via Direct Cleavage of the N≡N Bond

As described in the previous sections, molybdenum nitride complexes are considered as key reactive intermediates in the catalytic reduction of dinitrogen into ammonia. In the Schrock cycle and the catalytic cycle via dinuclear complexes, a terminal nitride complex is formed in six steps via stepwise protonation and reduction of the dinitrogen ligand (Scheme 12a). When the nitride complex is generated via direct cleavage of the bridging dinitrogen ligand in the catalytic cycle, the number of steps from the dinitrogen complex to the nitride complex decreases dramatically, and the catalytic activity increases (Scheme 12b).

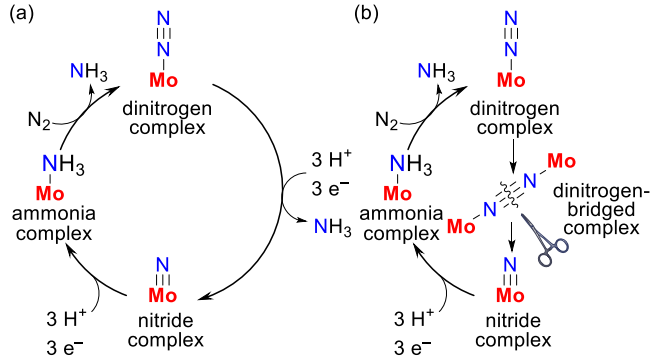

Scheme 12 Catalytic cycles of ammonia formation (a) via stepwise protonation and reduction of dinitrogen ligand (b) via direct cleavage of bridging dinitrogen ligand.

The first report on the generation of terminal nitride complex via direct cleavage of a bridging dinitrogen ligand was presented by Lapiaza and Cummins in 1995 (Scheme 13).[32] The reaction of molybdenum triamido complex [Mo(N(ᵗBu)Ar)₃] (Ar = 3,5-$C_6H_3Me_2$) with an atmospheric pressure of dinitrogen in diethyl ether at –35 °C afforded the dinitrogen-bridged dimolybdenum complex [{Mo(N(ᵗBu)Ar)₃}₂(μ-N_2)]. Increasing the reaction temperature to 30 °C gave the corresponding molybdenum nitride complex [Mo(N)(N(ᵗBu)Ar)₃] via direct cleavage of the bridging dinitrogen ligand. Since this report, the generation of terminal nitride complex via direct cleavage of dinitrogen ligand has been reported with various transition metals such as niobium,[33] molybdenum,[32,34] tungsten[35] and rhenium.[36]

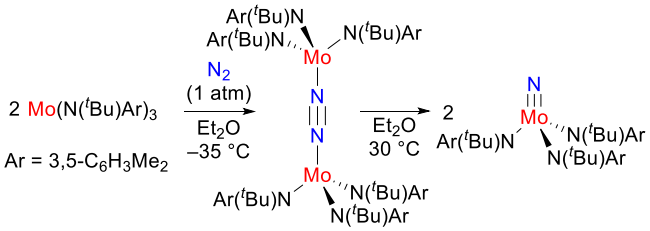

Scheme 13 First example of direct cleavage of bridged-dinitrogen ligand to afford terminal nitride complex.

Inspired by these researches, we investigated the direct cleavage of the dinitrogen ligand with our molybdenum complexes bearing a PNP-type pincer ligand.[19c,37] First, we performed the reduction of a molybdenum triiodide complex bearing a PNP ligand [MoI_3(PNP)] with 2.2 equivalents of $CoCp^*_2$ under an atmospheric pressure of dinitrogen at room temperature for 15 min to afford the corresponding nitride complex [MoI(N)(PNP)] in 90% NMR yield (Scheme 14). This result suggests that a nitride complex was formed via direct cleavage of the nitrogen–nitrogen triple bond of the bridging dinitrogen ligand in [MoI(PNP)–N≡N–MoI(PNP)]. This experimental result is in sharp contrast with the formation of [{$Mo(N_2)_2$(PNP)}₂(μ-N_2)] from the reaction of [$MoCl_3$(PNP)] with an excess amount of Na–Hg under an atmospheric pressure of dinitrogen at room temperature.[19a] To gain more insight on the reaction pathway, we carried out a stoichiometric reaction of [MoI_2(PNP)] derived from [MoI_3(PNP)] with 1 equivalent of $CoCp^*_2$ under an atmospheric pressure of dinitrogen at low temperature, obtaining the molybdenum(I) dinitrogen complex *trans*-[MoI(N_2)₂(PNP)] in 45% yield. The conversion of *trans*-[MoI(N_2)₂(PNP)] into [MoI(N)(PNP)] in toluene at room temperature was confirmed, demonstrating that *trans*-[MoI(N_2)₂(PNP)] was an intermediate in the formation of [MoI(N)(PNP)]. Separately, ammonia was formed from the reaction of [MoI(N)(PNP)] with 3 equivalents of $CoCp^*_2$ and 4 equivalents of [ColH]OTf under an argon atmosphere. In this reaction, the direct release of ammonia from [MoI(N)(PNP)] in the presence of a reductant and a proton source was confirmed.

The catalytic activity of several molybdenum complexes bearing a PNP ligand is shown in Scheme 15.[19c,37] The reaction of an atmospheric pressure of dinitrogen with 180 equivalents of $CoCp^*_2$ and 240 equivalents of [ColH]OTf per molybdenum atom in the presence of a catalytic amount of [MoI_3(PNP)] in toluene at room temperature for 20 hours afforded 51 equivalents of ammonia per

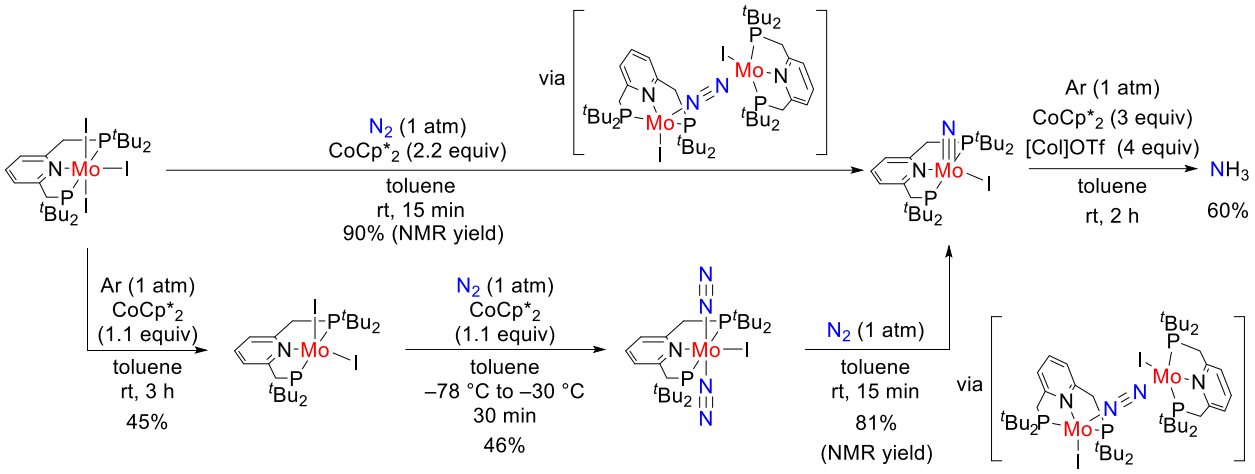

Scheme 14 Formation of nitride complex via direct cleavage of bridged-dinitrogen ligand on molybdenum complex bearing PNP pincer ligand.

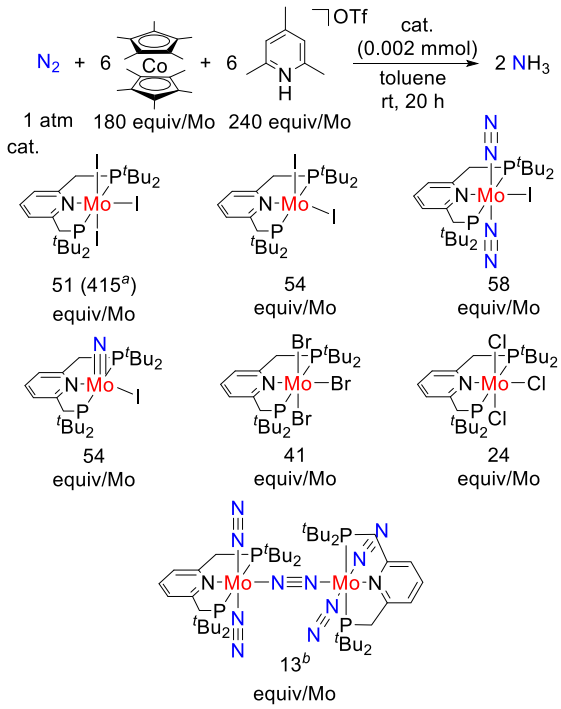

[a]Larger amounts of $CoCp^*_2$ (2160 equiv) and [ColH]OTf (2880 equiv) were used.
[b]Smaller amounts of $CoCp^*_2$ (108 equiv) and [ColH]OTf (144 equiv) were used.

Scheme 15 Catalytic ammonia formation using various molybdenum complexes bearing PNP-type pincer ligand.

molybdenum atom. The catalytic activity of [MoI_2(PNP)], *trans*-[$MoI(N_2)_2$(PNP)] and [MoI(N)(PNP)] was comparable to that of [MoI_3(PNP)] under the same reaction conditions. It is noteworthy that the catalytic activity of these complexes was higher than that of [{$Mo(N_2)_2$(PNP)}$_2$(μ-N_2)]. The catalytic activity of [MoX_3(PNP)] depended on the nature of the halide ligands, being the order of the catalytic activity as follows: [MoI_3(PNP)] > [$MoBr_3$(PNP)] > [$MoCl_3$(PNP)]. This tendency is comparable to the electron-donating ability of the halide ligands.[38] In fact, this tendency was supported by the cyclic voltammetry of the corresponding nitride complexes ([MoX(N)(PNP)]). These results suggest that reduction steps of the catalytic reaction by using [MoI_3(PNP)] proceed more smoothly than

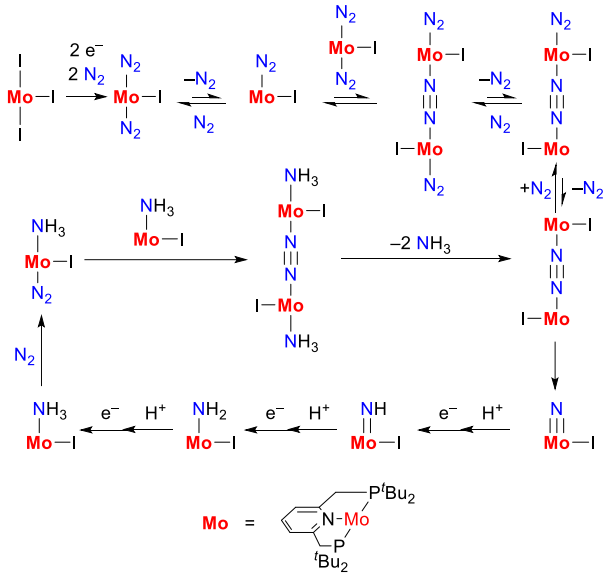

Scheme 16 Plausible reaction pathway via direct cleavage of bridged dinitrogen ligand.

those using [$MoBr_3$(PNP)] and [$MoCl_3$(PNP)]. The catalytic reaction using larger amounts of $CoCp^*_2$ and [ColH]OTf in the presence of [MoI_3(PNP)] as a catalyst gave up to 415 equivalents of ammonia per molybdenum atom.

A plausible reaction pathway for the catalytic reaction was proposed on the basis of experimental and theoretical results (Scheme 16).[19c,37] The catalytic cycle starts with the reduction of [MoI_3(PNP)] to form *trans*-[$MoI(N_2)_2$(PNP)]. According to DFT calculations, an equilibrium between *trans*-[$MoI(N_2)_2$(PNP)] and [MoI(PNP)–N≡N–MoI(PNP)] exists, accompanied by elimination of dinitrogen ligands and dimerization. In this equilibrium, *trans*-[$MoI(N_2)_2$(PNP)] is thermodynamically more favourable than [MoI(PNP)–N≡N–MoI(PNP)] by 12.6 kcal/mol. The highest activation energy of the first elimination of dinitrogen ligand from dinitrogen-bridged complex [$Mo(N_2)$I(PNP)–N≡N–$Mo(N_2)$I(PNP)] to another dinitrogen-bridged complex, i.e., [$Mo(N_2)$I(PNP)–N≡N–MoI(PNP)], was estimated to be 15.9 kcal/mol. Then, direct cleavage of the bridged dinitrogen ligand on [MoI(PNP)–N≡N–MoI(PNP)], which is a minor species in the

thermal equilibrium, occurs at room temperature to generate the corresponding nitride complex [MoI(N)(PNP)] ($\Delta G^{\ddagger}$ = 21.8 kcal/mol). Ammonia complex [MoI(NH_3)(PNP)] is formed by stepwise protonation and reduction of [MoI(N)(PNP)] via imide complex ([MoI(NH)(PNP)]) and amide complex ([MoI(NH_2)(PNP)]). Finally, ammonia is released from dinitrogen-bridged ammonia complex [Mo(NH_3)I(PNP)–N≡N–Mo(NH_3)I(PNP)] after dimerization of [MoI(NH_3)(PNP)], and the starting complex [MoI(PNP)–N≡N–MoI(PNP)] is regenerated.

We investigated the effect of substitution at the 4-position of the PNP pyridine ring in [MoI_3(PNP)] on the catalytic reaction via direct cleavage of nitrogen–nitrogen triple bond (Scheme 17).[39] The introduction of electron-deficient substituents such as the phenyl group resulted in higher catalytic activity. This tendency is in sharp contrast with that observed for the dinitrogen-bridged dimolybdenum catalysts shown in Scheme 9. These results indicate that the rate-limiting step of the catalytic reaction involving direct cleavage of the dinitrogen triple bond is not protonation but reduction. In addition, complexes having Fc and ruthenocenyl groups as redox active moieties showed higher catalytic activity, which suggests that the introduction of a redox active moiety accelerates the rate-determining reduction step in the catalytic cycle. We also investigated the catalytic activity of molybdenum triiodide complexes bearing a PNP ligand containing various substituents on the two phosphorus atoms, finding that bulky substituents play an important role, as previously described for the reaction system shown in Scheme 9.

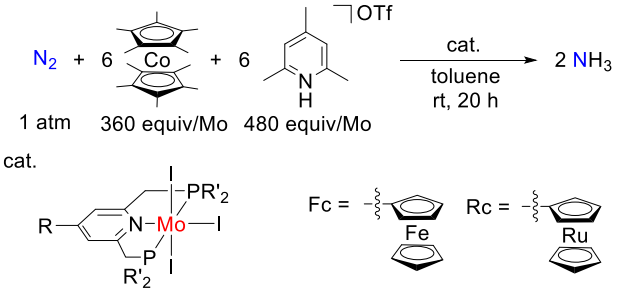

R	R'	NH_3 (equiv/Mo)
H	^{t}Bu	66 (10.9[a])
Ph	^{t}Bu	75
Me	^{t}Bu	49
MeO	^{t}Bu	20
Fc	^{t}Bu	83
Rc	^{t}Bu	75

R	R'	NH_3 (equiv/Mo)
H	Ad	8.4[a]
H	^{i}Pr	5.6[a]
H	Ph	1.9[a]

[a]36 equivalents of $CoCp_2$ and 48 equivalents of [LutH]OTf were used.

Scheme 17 Substituent effect on catalytic ammonia formation using various molybdenum triiodide complexes.

The catalytic activity of molybdenum trihalide complexes bearing a PCP-type pincer ligand was investigated under the same reaction conditions (Scheme 18).[40] Complexes of the type [MoX_3(PCP)] showed higher catalytic activity than the corresponding dinitrogen-bridged dimolybdenum complex [{Mo(N_2)$_2$(PCP)}$_2$(μ-N_2)] (Scheme 15). Interestingly, the addition of iodide ion to the reaction catalysed by [{Mo(N_2)$_2$(PCP)}$_2$(μ-N_2)] substantially improved the catalytic activity, which suggests that the catalytic reaction using [MoI_3(PCP)] may proceed via direct cleavage of the nitrogen–nitrogen triple bond of the bridging dinitrogen ligand as a key step. In contrast with the result for [{Mo(N_2)$_2$(PCP')}$_2$(μ-N_2)], which exhibited no catalytic activity (Scheme 11), the catalytic activity of molybdenum trihalide complexes bearing the PCP' ligand was similar to that of [MoX_3(PCP)]. We believe that the catalytic reaction using [MoX_3(PCP')] as catalysts proceeds via direct cleavage of the triple bond of the dinitrogen ligand as a key step.

Recently, we reported the first successful example of catalytic

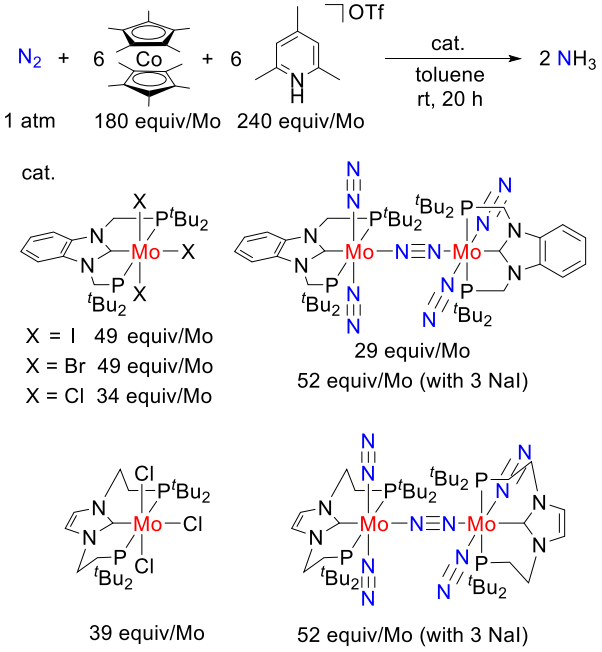

Scheme 18 Catalytic ammonia formation using molybdenum complexes bearing PCP-type pincer ligands.

formation of ammonia using alcohol or water as mild, abundant, and easily available proton sources and samarium diiodide (SmI_2) as a reductant (Scheme 19).[19d,41] The reaction of an atmospheric pressure of dinitrogen with 180 equivalents of SmI_2 and 180 equivalents of ethylene glycol per molybdenum atom in the presence of a catalytic amount of [MoI_3(PNP)] in THF at room temperature for 18 hours afforded 42.8 equivalents of ammonia per molybdenum atom. A time course study revealed that this reaction was completed within 30 min, with formation of 21.7 equivalents of ammonia within the initial 1 min (TOF = 21.7 equiv/Mo min^{-1}). The catalytic activity of [$MoBr_3$(PNP)] and [$MoCl_3$(PNP)] was slightly higher than that of [MoI_3(PNP)]. Dinitrogen-bridged dimolybdenum complex [{Mo(N_2)$_2$(PNP)}$_2$(μ-N_2)] was a less effective catalyst than molybdenum trihalide complexes [MoX_3(PNP)]. It is noteworthy that the catalytic reaction using molybdenum oxo complex [MoI(O)(H_2O)(PNP)][I] gave 44.1 equivalents of ammonia under the same reaction conditions. This result indicates that reactive species can be generated from molybdenum oxo complexes such as [MoI(O)(H_2O)(PNP)][I] under the catalytic reaction conditions. The catalytic activity of molybdenum complexes bearing the PCP ligand was higher than that of molybdenum complexes bearing the PNP ligand under the present reaction conditions using SmI_2 and ethylene glycol. Interestingly, water was a better proton source than ethylene glycol, affording a

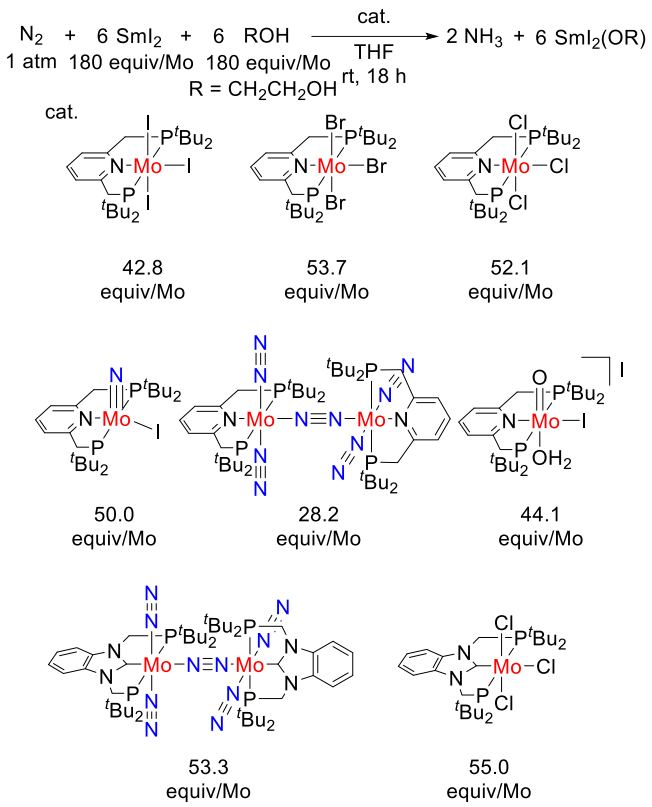

Scheme 19 Catalytic ammonia formation using SmI_2 and ethylene glycol.

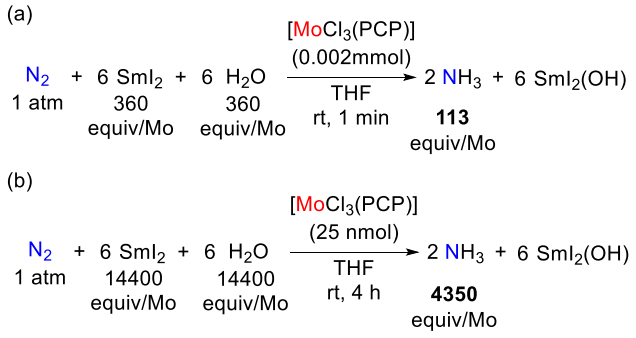

Scheme 20 Catalytic ammonia formation using SmI_2 and water.

reaction rate of 113 equiv/Mo min^{-1}, which is comparable to the reported values of nitrogenase enzyme,[7] and a maximum amount of ammonia of 4350 equivalents per molybdenum atom (Scheme 20).

According to the results of the stoichiometric reactions of $[MoX_3(PNP)]$ with SmI_2 under nitrogen to produce the corresponding nitride complex [MoI(N)(PNP)] (Scheme 21), it seems reasonable to conclude that the reaction using molybdenum complexes with pincer ligands as catalysts and SmI_2 as a reductant proceeds via direct cleavage of the triple bond of the dinitrogen ligand. As shown in Scheme 21, the stoichiometric reaction of [MoI(N)(PNP)] with 3 equivalents of SmI_2 and ethylene glycol under argon atmosphere gave ammonia quantitatively. However, no consumption of [MoI(N)(PNP)] was observed in the reaction with either SmI_2 or ethylene glycol. These results suggest that at least the first nitrogen–

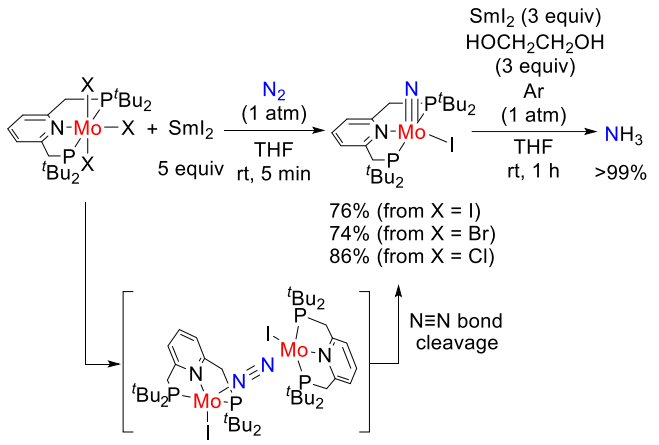

Scheme 21 Stoichiometric reactions of molybdenum complexes with SmI_2 and ethylene glycol.

hydrogen bond formation may proceed via proton-coupled electron transfer (PCET) process.[42] In many cases, the activation energy of the reaction via PCET is lower than that via stepwise proton/electron transfer process. As a result, the reaction via PCET proceeds more smoothly. Flowers' and Mayer's groups have found that reduction with SmI_2 and proton sources such as water or glycol proceeds via PCET process.[43,44,45] In these reaction systems, the coordination of proton sources to the samarium centre of SmI_2 weakens the X–H bond of the bound protic ligand. From these results, it can be concluded that the PCET process achieves high catalytic reactivity from the viewpoints of reaction rate and amount of ammonia production.

Chatt Cycle

As shown in the previous sections, the catalytic formation of ammonia can be divided into three types according to the reaction mechanism: the catalytic reaction via the Schrock cycle,[18,24,25] the reaction via the dinuclear reaction system,[19a,26,28] and the catalytic reaction via direct cleavage of the nitrogen–nitrogen triple bond of the dinitrogen ligand.[19c,19d,37] The catalytic reaction via the Chatt cycle shown in Scheme 3,[23] in contrast, was not developed until recently. On the basis of our recent findings on the reaction using SmI_2 and water or alcohol, we applied these conditions to the reaction catalysed by conventional molybdenum dinitrogen complexes bearing phosphines as auxiliary ligands, such as *trans*-$[Mo(N_2)_2(PMePh_2)_4]$ and *cis*-$[Mo(N_2)_2(PMe_2Ph)_4]$.[46] The reaction of an atmospheric

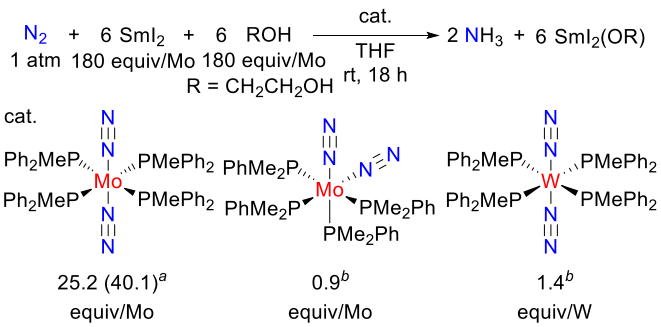

[a]Smaller amounts of SmI_2 (36 equiv) and ethylene glycol (36 equiv) were used.
[b]Water was used as a proton source instead of ethylene glycol.

Scheme 22 Catalytic ammonia formation using molybdenum-dinitrogen complexes bearing simple phosphines.

pressure of dinitrogen with 180 equivalents of SmI_2 and 180 equivalents of ethylene glycol per molybdenum atom in the presence of a catalytic amount of *trans*-$[Mo(N_2)_2(PMePh_2)_4]$ in THF at room temperature for 18 hours afforded 25.2 equivalents of ammonia per molybdenum atom (Scheme 22). In this reaction, water was more efficient as a proton source than ethylene glycol, affording 40.1 equivalents of ammonia per molybdenum atom. In contrast, *cis*-$[Mo(N_2)_2(PMe_2Ph)_4]$ and a similar tungsten dinitrogen complex, *trans*-$[W(N_2)_2(PMe_2Ph)_4]$, exhibited no catalytic activity under the same reaction conditions (Scheme 22). These experimental results prompted us to prepare in situ the molybdenum complexes from the reaction of $[MoI_3(THF)_3]$ with various phosphines, as shown in Scheme 23. A screening of phosphines revealed that 1,5-bis(diphenylphosphino)pentane was the best ligand, producing up to 82.9 equivalents of ammonia per molybdenum atom.

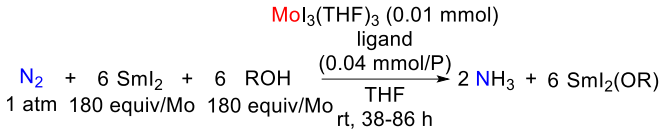

ligand	ROH = $HOCH_2CH_2OH$	ROH = H_2O
$PMePh_2$	24.3	40.0
$Ph_2P(CH_2)_5PPh_2$	39.7	46.1 (82.9)[a]

[a]Larger amounts of SmI_2 (360 equiv) and ethylene glycol (360 equiv) were used.

Scheme 23 Catalytic ammonia formation using molybdenum complexes.

A series of experiments were performed to shed some light on the reaction mechanism. The reaction of $[MoI_3(THF)_3]$ with 4 equivalents of $PMePh_2$ and 6 equivalents of SmI_2 in THF at room temperature for 18 h gave *trans*-$[Mo(N_2)_2(PMePh_2)_4]$ in 42% yield without formation of the corresponding nitride complexes (Scheme 24), indicating that no direct cleavage of the nitrogen–nitrogen triple bond of the bridging dinitrogen ligand occurred. This is in sharp contrast with the formation of the nitride complex from the reaction of *trans*-$[Mo(N_2)_2(depe)_2]$ (depe = 1,2-bis(diethylphosphino)ethane) with 1

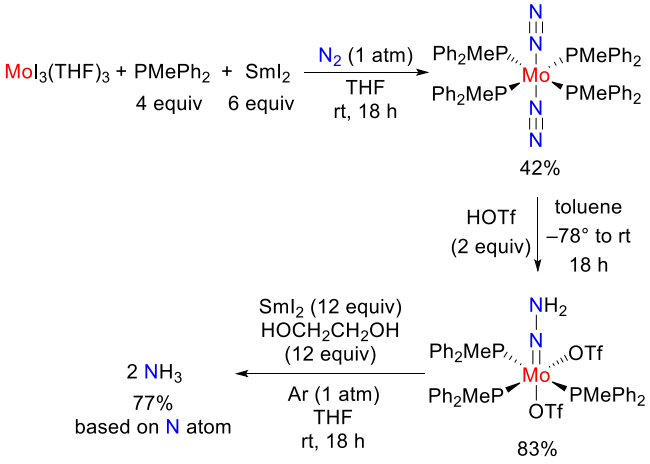

Scheme 24 Stoichiometric reactions of molybdenum-dinitrogen complex with SmI_2 and ethylene glycol.

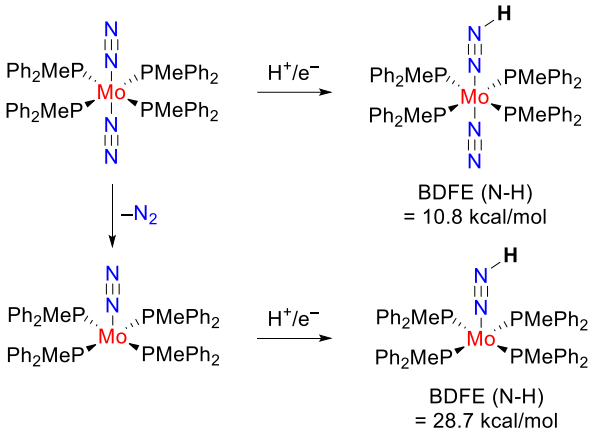

Scheme 25 DFT calculations of BDFE(N-H) of molybdenum diazenide complexes.

equivalent of oxidant via direct cleavage of the nitrogen–nitrogen triple bond of the bridging dinitrogen ligand.[34f] In fact, the stoichiometric reaction of hydrazide(2−) complex *cis*,*mer*-$[Mo(NNH_2)(OTf)_2(PMePh_2)_3]$, prepared from protonation of *trans*-$[Mo(N_2)_2(PMePh_2)_4]$ with 2 equivalents of HOTf, with SmI_2 and ethylene glycol under argon atmosphere gave ammonia in 77% yield based on the Mo atom. Separately, we confirmed that *cis*,*mer*-$[Mo(NNH_2)(OTf)_2(PMePh_2)_3]$ showed a catalytic activity similar to that of *trans*-$[Mo(N_2)_2(PMePh_2)_4]$.

DFT calculations supported the formation of an N–H bond via PCET process. The bond dissociation free energy (BDFE) values calculated in THF at 298 K for the N–H bond in related molybdenum diazenide complexes are shown in Scheme 25. The BDFE (N–H) of *trans*-$[Mo(N_2)(NNH)(PMePh_2)_4]$ was 10.8 kcal/mol, which was considerably smaller than the BDFE value of an O–H bond estimated for $SmI_2(H_2O)_n$ (26 kcal/mol).[45] Meanwhile, the BDFE (N–H) of molybdenum diazenide complex $[Mo(NNH)(PMePh_2)_4]$ was estimated to be 28.7 kcal/mol. These results suggest that hydrogen transfer may occur from $SmI_2(H_2O)_n$ or an SmI_2–ethylene glycol complex to the terminal dinitrogen ligand of $[Mo(N_2)(PMePh_2)_4]$. Considering the experimental and theoretical results, we believe that the catalytic reaction using *trans*-$[Mo(N_2)_2(PMePh_2)_4]$ as a catalyst proceeds via sequential N–H bond formation of the terminal dinitrogen ligand, with formation of a hydrazide(2−) complex as a key reactive intermediate. This can be considered as the first successful

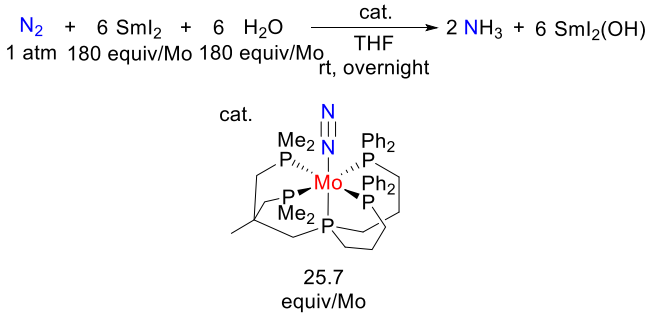

Scheme 26 Catalytic ammonia formation using molybdenum-dinitrogen complexes bearing pentadentate tetrapodal phosphine ligand.

example of catalytic ammonia formation via the Chatt-type cycle, although further investigation on the reaction mechanism is required.

Quite recently, Tuczek and co-workers reported that a molybdenum dinitrogen complex bearing a pentadentate tetrapodal phosphine ligand ([Mo(N$_2$)P$^{Me}_2$PP$^{Ph}_2$]) served as a catalyst for ammonia formation from the reaction with SmI_2 and water (Scheme 26).[20] The reaction of an atmospheric pressure of dinitrogen with 180 equivalents of SmI_2 and water in the presence of a catalytic amount of [Mo(N$_2$)P$^{Me}_2$PP$^{Ph}_2$] gave 25.7 equivalents of ammonia per molybdenum atom. The experimental and computational results point toward this reaction system as the second successful example of the catalytic ammonia formation via the Chatt cycle.

Outlook

Numerous catalytic reaction systems for nitrogen fixation using transition metal complexes as catalysts under mild reaction conditions have been reported in the last decade. Of particular interest is our novel reaction system for catalytic ammonia formation from nitrogen under ambient reaction conditions, which proceeds via direct cleavage of the nitrogen–nitrogen triple bond of a bridging dinitrogen ligand as a key step of the catalytic cycle. In the reaction using SmI_2 as reductant and water as proton source, molybdenum complexes bearing a PCP-type pincer ligand proved to be the most effective catalysts. A high catalytic activity, comparable to that obtained with nitrogenase enzyme, was achieved. However, further investigation is required to develop a next generation of catalysts for nitrogen fixation that can replace the Haber–Bosch process.

Table 1 Chemical overpotentials with combination of reductants and proton sources.[a]

$$1/2\ N_2 + 3\ H^+ + 3\ e^- \longrightarrow NH_3$$

$$\Delta\Delta G_f(NH_3) = 3(\Delta G_f^\circ(H\cdot) - BDFE)$$
$$BDFE_{eff} = 1.37(pK_a) + 23.06(E_{red}) + C_G$$

$\Delta\Delta G_f(NH_3)$:chemical overpotential (kcal/mol)
$BDFE_{eff}$: effective bond dissociation energy (kcal/mol)
$\Delta G_f^\circ(H\cdot)$: standard Gibbs energy of formation of H·

reductant	$E_{1/2}^\circ$ in MeCN	proton source	pK_a in MeCN	$BDFE_{eff}$	$\Delta\Delta G_f(NH_3)$
KC_8	–3.24	$[(Et_2O)_2H]^+$	1.32	(0)	156
KC_8	–3.24	$[PCy_3H]^+$	16.1	(0)	156
$CoCp^*_2$	–1.91	$[Ph_2NH_2]^+$	5.98	16.7	106
$SmI_2(H_2O)_n$		$[SmI_2(H_2O)_n]^+$		26[b]	78
$CoCp^*_2$	–1.91	$[LutH]^+$	14.16	27.9	72
$CoCp^*_2$	–1.91	$[ColH]^+$	15.00	29.0	69
$CrCp^*_2$	–1.45	$[LutH]^+$	14.16	38.5	41
$CoCp_2$	–1.32	$[LutH]^+$	14.16	41.5	32

[a]$BDFE_{eff}$ and $\Delta\Delta G_f^\circ$ values are calculated from $E_{1/2}^\circ$ (KC_8,[49,50] $CoCp^*_2$,[51] $CrCp^*_2$,[52] and $CoCp_2$[52]) and pK_a values ($[(Et_2O)_2H]^+$,[53] $[PCy_3H]^+$,[54] $[Ph_2NH_2]^+$,[55] $[LutH]^+$,[55] and $[ColH]^+$ [55]) in MeCN at 25 °C with C_G[56] and $\Delta G_f^\circ(H\cdot)$[56] values. [b]The $BDFE_{eff}$ values of $SmI_2(H_2O)_n$ was estimated by Mayer and co-workers by using $E_{1/2}^\circ$ of $Sm(H_2O)_n^{2+}$(aq) and pKa values of $[Eu(H_2O)_n]^{3+}$(aq).[45,57]

As described in the present paper, the combination of reductants and proton sources consumes higher energy than is ideally required for ammonia production.[10-21] The excess energy required for ammonia production is calculated as chemical overpotentials on the basis of effective bond dissociation free energy ($BDFE_{eff}$). Chirik and co-workers have defined chemical overpotentials in the transition metal-catalysed formation of ammonia using a reductant and a proton source as an excess thermodynamic driving force in comparison with ammonia production from hydrogen gas.[47,48] Chemical overpotential values of the combinations of reductants and proton sources for ammonia production are summarized in Table 1. As can be seen, combinations such as $CoCp^*_2$/$[ColH]^+$ or SmI_2/H_2O have relatively high chemical overpotential values for ammonia production. Accordingly, the exploration of more effective combinations of reductants and proton sources with lower chemical overpotentials seems an obvious and challenging future research topic.

We believe that the development of nitrogen fixation using the energy of visible light is an important research topic from the viewpoint of sustainable chemistry. In fact, our group reported catalytic ammonia formation using proton sources generated from water assisted by photoredox catalysts under visible light.[58] Although this is not an ideal system because reductants are not generated from the energy of visible light, it constitutes a successful example of ammonia formation in a photoredox reaction system. In 2019, Chirik and Knowles reported the photoredox-assisted formation of ammonia from a manganese nitride complex with 1,10-dihydroacridine acting as both reductant and proton source.[59] Further investigation of novel photoredox-catalysed reaction systems using the energy of visible light is, therefore, another challenging subject.

The development of nitrogen fixation using renewable energy such as solar, wind or geothermal power is also an important research topic in terms of sustainable chemistry. To achieve this goal, the formation of ammonia should proceed under electrochemical conditions without reductants. Although electrochemical ammonia formation catalysed by transition metal complexes have been reported, the faraday efficiency of these reactions was quite low.[60] Nonetheless, Peters and co-workers have recently reported the electrochemical formation of ammonia using an iron complex as a catalyst with high faraday efficiency.[61] Therefore, the development of highly efficient reaction systems under electrochemical conditions for practical purposes deserves special research attention.[62]

Conflicts of interest

There are no conflicts to declare.

Acknowledgements

The present project is supported by CREST, JST (Grant JPMJCR1541). We acknowledge Grants-in-Aid for Scientific Research (Grants JP17H01201, 18K19093, 20H05671, and 20K21203) from JSPS and MEXT. Y.A. is a recipient of the JSPS Research Fellowships for Young Scientists.

Notes and references

1.*Mineral Commodity Summaries 2020*, U.S. Geological Survey, 2020.
2. L. K. Boerner, *Chem. Eng. News*, 2019, **97**, 18–21.
3. (a) J. Guo and P. Chen, *Chem*, 2017, **3**, 709–712; (b) L. Ye, R. Nayak-Luke, R. Bañares-Alcántara and E. Tsang, *Chem*, 2017, **3**, 712–714; (c) S. Giddey, S. P. S. Badwal, C. Munnings and M. Dolan, *ACS Sustainable Chem. Eng.*, 2017, **5**, 10231–10239.
4. (a) H. Liu, *Ammonia Synthesis Catalysts, Innovation and Practice*; Chemical Industry Press and World Scientific: Singapore and Beijing, 2013; (b) M. Appl, in *Ullmann's Encyclopedia of Industrial Chemistry*; Wiley-VCH: Weinheim, 7th ed., 2011, vol. 7, pp. 107–261.
5. (a) *Catalysts for Nitrogen Fixation: Nitrogenases, Relevant Chemical Models and Commercial Processes*; eds. B. E. Smith, R. L. Richards and W. E. Newton, Kluwer Academic Publishers: Berlin, 2004; (b) *Nitrogen Fixation: Methods and Protocols*; ed. M. W. Ribbe, Humana Press: Totowa, 2011.
6. (a) O. Einsle and D. C. Rees, *Chem. Rev.*, 2020, **120**, 4969–5004; (b) C. Van Stappen, L. Decamps, G. E. Cutsail III, R. Bjornsson, J. T. Henthorn, J. A. Birrell and S. DeBeer, *Chem. Rev.*, 2020, **120**, 5005–5081; (c) L. C. Seefeldt, Z.-Y. Yang, D. A. Lukoyanov, D. F. Harris, D. R. Dean, S. Raugei and B. M. Hoffman, *Chem. Rev.*, 2020, **120**, 5082–5106; (d) A. J. Jasniewski, C. C. Lee, M. W. Ribbe and Y. Hu, *Chem. Rev.*, 2020, **120**, 5107–5157; (e) H. L. Rutledge and F. A. Tezcan, *Chem. Rev.*, 2020, **120**, 5158–5193.
7. (a) B. J. Hales and E. E. Case, *J. Biol. Chem.*, 1987, **262**, 16205–16211; (b) J. R. Chisnell, R. Premakumar and P. E. Bishop, *J. Bacteriol.*, 1988, **170**, 27–33; (c) J. Christiansen, V. L. Cash, L. C. Seefeldt and D. R. Dean, *J. Biol. Chem.*, 2000, **275**, 11459–11464; (d) C. C. Lee, Y. Hu and M. W. Ribbe, *Proc. Natl. Acad. Sci. U. S. A.*, 2009, **106**, 9209–9214; (e) K. A. Brown, D. F. Harris, M. B. Wilker, A. Rasmussen, N. Khadka, H. Hamby, S. Keable, G. Dukovic, J. W. Peters, L.C. Seefeldt and P. W. King, *Science*, 2016, **352**, 448–450; (f) D. F. Harris, D. A. Lukoyanov, H. Kallas, C. Trncik, Z.-Y. Yang, P. Compton, N. Kelleher, O. Einsle, D. R. Dean, B. M. Hoffman and L. C. Seefeldt, *Biochemistry*, 2019, **58**, 3293–3301.
8. (a) *Nitrogen Fixation (Topics in Organometallic Chemistry 60)*, ed. Y. Nishibayashi, Springer, Cham, 2017; (b) *Transition Metal−Dinitrogen Complexes: Preparation and Reactivity*; ed. Y. Nishibayashi, Wiley-VCH: Weinheim, 2019.
9. (a) K. C. MacLeod and P. L. Holland, *Nat. Chem.*, 2013, **5**, 559–565; (b) H.-P. Jia and E. A. Quadrelli, *Chem. Soc. Rev.*, 2014, **43**, 547–564; (c) C. J. M. van der Ham, M. T. M. Koper and D. G. H. Hetterscheid, *Chem. Soc. Rev.*, 2014, **43**, 5183–5191; (d) C. Sivasankar, S. Baskaran, M. Tamizmani and K. J. Ramakrishna, *Organomet. Chem.*, 2014, **752**, 44–58; (e) D. R. Z. Tyler, *Anorg. Allg. Chem.*, 2015, **641**, 31–39; (f) N. Khoenkhoen, B. de Bruin, J. N. H. Reek and W. I. Dzik, *Eur. J. Inorg. Chem.*, 2015, **2015**, 567–598; (g) H. Tanaka, Y. Nishibayashi and K. Yoshizawa, *Acc. Chem. Res.*, 2016, **49**, 987–995; (h) Y. Ohki and H. Seino, *Dalton Trans.*, 2016, **45**, 874–880; (i) B. M. Flöser and F. Tuczek, *Coord. Chem. Rev.*, 2017, **345**, 263–280; (j) R. J. Burford and M. D. Fryzuk, *Nat. Chem. Rev.*, 2017, **1**, 0026; (k) S. L. Foster, S. I. P. Bakovic, R. D. Duda, S. Maheshwari, R. D. Milton, S. D. Minteer, M. J. Janik and J. N. Renner, *Nat. Catal.*, 2018, **1**, 490–500; (l) N. Stucke, B. M. Flöser, T. Weyrich and F. Tuczek, *Eur. J. Inorg. Chem.*, 2018, **2018**, 1337–1355; (m) Y. Nishibayashi, *Dalton Trans.*, 2018, **47**, 11290–11297; (n) Y. Tanabe and Y. Nishibayashi, *Coord. Chem. Rev.*, 2019, 389, 73–93; (o) M. J. Chalkley and J. C. Peters, *Eur. J. Inorg. Chem.*, 2020, **2020**, 1353–1357; (p) A. J. Kendall and M. T. Mock, *Eur. J. Inorg. Chem.*, 2020, **2020**, 1358–1375; (q) C. Sivasankar, P. K. Madarasi and M. Tamizmani, *Eur. J. Inorg. Chem.*, 2020, **2020**, 1383–1395; (r) M. J. Chalkley, M. W. Drover and J. C. Peters, *Chem. Rev.*, 2020, **120**, 5582–5639; (s) K. Tanifuji and Y. Ohki, *Chem. Rev.*, 2020, **120**, 5194–5251; (t) D. Singh, W. R. Buratto, J. F. Torres and L. J. Murray, *Chem. Rev.*, 2020, **120**, 5517–5581.
10. L. R. Doyle, A. J. Wooles, L. C. Jenkins, F. Tuna, E. J. L. McInnes and S. T. Liddle, *Angew. Chem., Int. Ed.*, 2018, **57**, 6314–6318.
11. Y. Sekiguchi, K. Arashiba, H. Tanaka, A. Eizawa, K. Nakajima, K. Yoshizawa and Y. Nishibayashi, *Angew. Chem., Int. Ed.*, 2018, **57**, 9064–9068.
12. Y. Kokubo, Y. Wasada-Tsutsui, S. Yomura, S. Yanagisawa, M. Kubo, S. Kugimiya, Y. Kajita, T. Ozawa and H. Masuda, *Eur. J. Inorg. Chem.*, 2020, **2020**, 1456–1464.
13. (a) J. S. Adnerson, J. Rittle and J. C. Peters, *Nature*, 2013, **501**, 84–87; (b) G. Ung and J. C. Peters, *Angew. Chem., Int. Ed.*, 2015, **54**, 532–535; (c) T. J. Del Castillo, N. B. Thompson and J. C. Peters, *J. Am. Chem. Soc.*, 2016, **138**, 5341–5350; (d) T. M. Buscagan, P. H. Oyala and J. C. Peters, *Angew. Chem., Int. Ed.*, 2017, **56**, 6921–6926; (e) M. J. Chalkley, T. J. Del Castillo, B. D. Matson, J. P. Roddy and J. C. Peters, *ACS Cent. Sci.*, 2017, **3**, 217–223.
14. (a) S. Kuriyama, K. Arashiba, K. Nakajima, Y. Matsuo, H. Tanaka, K. Ishii, K. Yoshizawa and Y. Nishibayashi, *Nat. Commun.*, 2016, **7**, 12181; (b) Y. Sekiguchi, S. Kuriyama, A. Eizawa, K. Arashiba, K. Nakajima and Y. Nishibayashi, *Chem. Commun.*, 2017, **53**, 12040–12043; (c) J. Higuchi, S. Kuriyama, A. Eizawa, K. Arashiba, K. Nakajima and Y. Nishibayashi, *Dalton Trans.*, 2018, **47**, 1117–1121.
15. P. J. Hill, L. R. Doyle, A. D. Crawford, W. K. Myers and A. E. Ashley, *J. Am. Chem. Soc.*, 2016, **138**, 13521–13524.
16. S. Kuriyama, K. Arashiba, H. Tanaka, Y. Matsuo, K. Nakajima, K. Yoshizawa and Y. Nishibayashi, *Angew. Chem., Int. Ed.*, 2016, **55**, 14291–14295.
17. T. J. Del Castillo, N. B. Thompson, D. L. Suess, G. Ung and J. C. Peters, *Inorg. Chem.*, 2015, **54**, 9256–9262.
18. (a) D. V. Yandulov and R. R. Schrock, *Science*, 2003, **301**, 76–78; (b) V. Ritleng, D. V. Yandulov, W. W. Weare, R. R. Schrock, A. S. Hock and W. M. Davis, *J. Am. Chem. Soc.*, 2004, **126**, 6150–6163; (c) L. A. Wickramasinghe, T. Ogawa, R. R. Schrock and P. Müller, *J. Am. Chem. Soc.*, 2017, **139**, 9132–9135.
19. (a) K. Arashiba, Y. Miyake and Y. Nishibayashi, *Nat. Chem.*, 2011, **3**, 120–125; (b) A. Eizawa, K. Arashina, H. Tanaka, S. Kuriyama, Y. Matsuo, K. Nakajima, K. Yoshizawa and Y. Nishibayashi, *Nat. Commun.*, 2017, **8**, 14874; (c) K. Arashiba, A. Eizawa, H. Tanaka, K. Nakajima, K. Yoshizawa and Y. Nishibayashi, *Bull. Chem. Soc. Jpn.*, 2017, **90**, 1111–1118; (d) Y. Ashida, K. Arashiba, K. Nakajima and Y. Nishibayashi, *Nature*, 2019, **568**, 536–540.
20. T. A. Engesser, A. Kindjajev, J. Junge, J. Krahmer and F. Tuczek, *Chem. − Eur. J.*, 2020, DOI: 10.1002/chem.202003549.
21. J. Fajardo and J. C. Peters, *J. Am. Chem. Soc.*, 2017, **139**, 16105–16108.

22. (a) J. Chatt, A. J. Pearman and R. L. Richards, *Nature*, 1975, **253**, 39–40; (b) J. Chatt, A. J. Pearman and R. L. J. Richards, *Chem. Soc., Dalton Trans.*, 1977, 1852–1860.
23. (a) J. Chatt and R. L. Richards, *J. Organomet. Chem.*, 1982, **239**, 65−77; (b) C. J. Pickett, *JBIC*, 1996, **1**, 601−606; (c) F. Barrière, *Coord. Chem. Rev.*, 2003, **236**, 71−89; (d) F. Tuczek, K. H. Horn and N. Lehnert, *Coord. Chem. Rev.*, 2003, **245**, 107−120; (e) G. C. Stephan, C. Sivasankar, F. Studt and F. Tuczek, *Chem. − Eur. J.*, 2008, **14**, 644−652; (f) A. Dreher, G. Stephan and F. Tuczek, *Adv. Inorg. Chem.*, 2009, **61**, 367−405.
24. (a) R. R. Schrock, *Acc. Chem. Res.*, 2005, **38**, 955−962; (b) R. R. Schrock, *Angew. Chem., Int. Ed.*, 2008, **47**, 5512−5522.
25. (a) D. V. Yandulov and R. R. Schrock, *J. Am. Chem. Soc.*, 2002, **124**, 6252−6253; (b) D. V. Yandulov, R. R. Schrock, A. L. Rheingold, C. Ceccarelli and W. M. Davis, *Inorg. Chem.*, 2003, **42**, 796−813; (c) D. V. Yandulov and R. R. Schrock, *Inorg. Chem.*, 2005, **44**, 1103−1117; (d) W. W. Weare, X. Dai, M. J. Byrnes, J. M. Chin and R. R. Schrock, *Proc. Natl. Acad. Sci. U. S. A.*, 2006, **103**, 17099−17106; (e) V. Ritleng, D. V. Yandulov, W. W. Weare, R. R. Schrock, A. S. Hock and W. M. Davis, *J. Am. Chem. Soc.*, 2004, **126**, 6150−6163.
26. H. Tanaka, K. Arashiba, S. Kuriyama, A. Sasada, K. Nakajima, K. Yoshizawa and Y. Nishibayashi, *Nat. Commun.*, 2014, **5**, 3737.
27. Y.-H. Tian, A. W. Pierpont and E. R. Batista, *Inorg. Chem.*, 2014, **53**, 4177−4183.
28. A. Egi, H. Tanaka, A. Konomi, Y. Nishibayashi and K. Yoshizawa, *Eur. J. Inorg. Chem.*, 2020, **2020**, 1490−1498.
29. (a) S. Kuriyama, K. Arashiba, K. Nakajima, H. Tanaka, N. Kamaru, K. Yoshizawa and Y. Nishibayashi, *J. Am. Chem. Soc.*, 2014, **136**, 9719−9731; (b) S. Kuriyama, K. Arashiba, K. Nakajima, H. Tanaka, K. Yoshizawa and Y. Nishibayashi, *Chem. Sci.*, 2015, **6**, 3940−3951.
30. E. Kinoshita, K. Arashiba, S. Kuriyama, Y. Miyake, R. Shimazaki, H. Nakanishi and Y. Nishibayashi, *Organometallics*, 2012, **31**, 8437−8443.
31. K. Arashiba, E. Kinoshita, S. Kuriyama, A. Eizawa, K. Nakajima, H. Tanaka, K. Yoshizawa and Y. Nishibayashi, *J. Am. Chem. Soc.*, 2015, **137**, 5666−5669.
32. C. E. Laplaza and C. C. Cummins, *Science*, 1995, **268**, 861−863.
33. D. J. Mindiola, K. Meyer, J.-P. F. Cherry, T. A. Baker and C. C. Cummins, *Organometallics*, 2000, **19**, 1622−1624.
34. (a) C. Rebreyend and B. de Bruin, *Angew. Chem., Int. Ed.*, 2015, **54**, 42−44; (b) T. J. Hebden, R. R. Schrock, M. K. Takase and P. Müller, *Chem. Commun.*, 2012, **48**, 1851−1853; (c) T. Miyazaki, H. Tanaka, Y. Tanabe, M. Yuki, K. Nakajima, K. Yoshizawa and Y. Nishibayashi, *Angew. Chem., Int. Ed.*, 2014, **53**, 11488−11492; (d) Q. Liao, A. Cavaillé, N. Saffon-Merceron and N. Mézailles, *Angew. Chem., Int. Ed.*, 2016, **55**, 11212−11216; (e) G. A. Silantyev, M. Förster, B. Schluschaß, J. Abbenseth, C. Würtele, C. Volkmann, M. C. Holthausen and S. Schneider, *Angew. Chem., Int. Ed.*, 2017, **56**, 5872−5876; (f) A. Katayama, T. Ohta, Y. Wasada-Tsutsui, T. Inomata, T. Ozawa, T. Ogura and H. Masuda, *Angew. Chem., Int. Ed.*, 2019, **58**, 11279–11284; (g) S. Bennaamane, M, F, Espada, I. Yagoub, N. Saffon-Merceron, N. Nebra, M. Fustier-Boutignon, E. Clot and N. Mézailles, *Eur. J. Inorg. Chem.*, 2020, **2020**, 1499−1505; (h) J. Abenseth, J.-P. H. Oudsen, B. Venderbosch, S. Demeshko, M. Finger, C. Herwig, C. Würtele, M. C. Holthausen, C. Limberg, M. Tromp and S. Schneider, *Inorg. Chem*, 2020, **59**, 14367−14375.
35. B. Schluschaß, J. Abbenseth, S. Demeshko, M. Finger, A. Franke, C. Herwig, C. Würtele, I. Ivanovic-Burmazovic, C. Limberg, J. Telser and S. Schneider, *Chem. Sci.*, 2019, **10**, 10275−10282.
36. (a) M. J. Bezdek and P. J. Chirik, *Angew. Chem., Int. Ed.*, 2016, **55**, 7892−7896; (b) I. Klopsch, M. Finger, C. Würtele, B. Milde, D. B. Werz and S. Schneider, *J. Am. Chem. Soc.*, 2014, **136**, 6881−6883; (c) Q. J. Bruch, G. P. Connor, C.-H. Chen, P. L. Holland, J. M. Mayer, F. Hasanayn and A. J. M. Miller, *J. Am. Chem. Soc.*, 2019, **141**, 20198−20208; (d) R. S. van Alten, F. Wätjen, S. Demeshko, A. J. M. Miller, C. Würtele, I. Siewert and S. Schneider, *Eur. J. Inorg. Chem.*, 2020, **2020**, 1402−1410.
37. K. Arashiba, H. Tanaka, K. Yoshizawa and Y. Nishibayashi, *Chem. − Eur. J.*, 2020, **26**, 13383−13389.
38. K. Fagnou, and M. Lautens, *Angew. Chem., Int. Ed.*, 2002, **41**, 26−47.
39. T. Itabashi, I. Mori, K. Arashiba, A. Eizawa, K. Nakajima and Y. Nishibayashi, *Dalton Trans.*, 2019, **48**, 3182−3186.
40. A. Eizawa, K. Arashiba, A. Egi, H. Tanaka, K. Nakajima, K. Yoshizawa and Y. Nishibayashi, *Chem. Asian J.*, 2019, **14**, 2091−2096.
41. Y. Ashida, S. Kondo, K. Arashiba, T. Kikuchi, K. Nakajima, S. Kakimoto and Y. Nishibayashi, *Synthesis*, 2019, **51**, 3792−3795.
42. (a) J. J. Warren, T. A. Tronic and J. M. Mayer, *Chem. Rev.*, 2010, **110**, 6961−7001; (b) D. R. Weinberg, C. J. Gagliardi, J. F. Hull, C. F. Murphy, C. A. Kent, B. C. Westlake, A. Paul, D. H. Ess, D. G. McCafferty and T. J. Meyer, *Chem. Rev.*, 2012, **112**, 4016−4093; (c) D. C. Miller, K. T. Tarantino and R. R. Knowles, *Top. Curr. Chem.*, 2016, **374**, 30.
43. C. O. Bartulovich and R. A. Flowers, II, *Dalton Trans.*, 2019, **48**, 16142−16147.
44. (a) T. V. Chciuk and R. A. Flowers, II, *J. Am. Chem. Soc.*, 2015, **137**, 11526−11531; (b) T. V. Chciuk, W. R. Anderson, Jr. and R. A. Flowers, II, *J. Am. Chem. Soc.*, 2016, **138**, 8738−8741; (c) T. V. Chciuk, W. R. Anderson, Jr. and R. A. Flowers, II, *Angew. Chem., Int. Ed.*, 2016, **55**, 6033−6036; (d) T. V. Chciuk, A. M. Li, A. Vazquez-Lopez, W. R. Anderson, Jr. and R. A. Flowers, II, *Org. Lett.*, 2017, **19**, 290−293; (e) T. V. Chciuk, W. R. Anderson, Jr. and R. A. Flowers, II, *J. Am. Chem. Soc.*, 2018, **140**, 15342−15352.
45. S. S. Kolmar and J. M. Mayer, *J. Am. Chem. Soc.*, 2017, **139**, 10687−10692.
46. Y. Ashida, K. Arashiba, H. Tanaka, A. Egi, K. Nakajima, K. Yoshizawa and Y. Nishibayashi, *Inorg. Chem.*, 2019, **58**, 8927−8932.
47. M. J. Bezdek, I. Pappas and P. J. Chirik, *Nitrogen Fixation (Topics in Organometallic Chemistry)*, ed. Y. Nishibayashi, Springer, Cham, 2017, vol. 60, pp. 1−22.
48. (a) M. J. Bezdek, S. Guo and P. J. Chirik, *Science*, 2016, **354**, 730−733; (b) I. Pappas and P. J. Chirik, *J. Am. Chem. Soc.*, 2016, **138**, 13379−13389; (c) M. J. Bezdek and P. J. Chirik, *Angew. Chem., Int. Ed.*, 2018, 57, 2224−2228.
49. The value for KC_8 in MeCN is based on the intercalation voltage of graphite vs K^+/K (240 mV) taken from ref. 49.
50. Z. Jian, W. Luo and X. Ji, *J. Am. Chem. Soc.*, 2015, **137**, 11566–11569.

51. J. R. Aranzaes, M.-C. Daniel and D. Astruc, *Can. J. Chem.*, 2006, **84**, 288–299.
52. J. L. Robbins, N. Edelstein, B. Spencer and J. C. Smart, *J. Am. Chem. Soc.*, 1982, **104**, 1882–1893.
53. I. M. Kolthoff and M. K. Chantooni, Jr., *J. Am. Chem. Soc.*, 1968, **90**, 3320–3326.
54. (*a*) K. Abdur-Rashid, T. P. Fong, B. Greaves, D. G. Gusev, J. G. Hinman, S. F. Landau, A. L. Lough and R. H. Morris, *J. Am. Chem. Soc.*, 2000, **122**, 9155–9171; (*b*) J.-N. Li, Y. Fu, L. Liu and Q.-X. Guo, *Tetrahedron*, 2006, **62**, 11801–11813.
55. I. Kaljurand, A. Kütt, L. Sooväli, T. Rodima, V. Mäemets, I. Leito and I. A. Koppel, *J. Org. Chem.*, 2005, **70**, 1019–1028.
56. C. F. Wise, R. G. Agarwal and J. M. Mayer, *J. Am. Chem. Soc.*, 2020, **142**, 10681–10691.
57. The authors of this manuscript understood that the calculation of the $BDFE_{eff}$ values should be estimated from the pKa and redox potential of $[SmI_2(H_2O)_n]$ in THF. However, unfortunately, the pKa value of $[SmI_2(H_2O)_n]$ in THF has not been reported until now. As a result, in this paper, the authors used the $BDFE_{eff}$ value of $[SmI_2(H_2O)_n]$ in water estimated by Mayer's group.[45]
58. Y. Tanabe, K. Arashiba, K. Nakajima and Y. Nishibayashi, *Chem. Asian J.*, 2017, **12**, 2544–2548.
59. (a) D. Wang, F. Loose, P. J. Chirik and R. R. Knowles, *J. Am. Chem. Soc.*, 2019, **141**, 4795−4799; (b) F. Loose, D. Wang, L. Tian, G. D. Scholes, R. R. Knowles and P. J. Chirik, *Chem. Commun.*, 2019, **55**, 5595−5598.
60. G. Qing, R. Ghazfar, S. T. Jackowski, F. Habibzadeh, M. Maleka Ashtiani, C.-P. Chen, M. R. Smith, III and T. W. Hamann, *Chem. Rev.*, 2020, **120**, 5437–5516.
61. M. J. Chalkley, T. J. Del Castillo, B. D. Matson and J. C. Peters, *J. Am. Chem. Soc.*, 2018, **140**, 6122−6129.
62. K. Arashiba, R. Kenega, Y. Himeda and Y. Nishibayashi, *Chem. Lett.*, **2020**, *49*, 1171-1173.

brief biographies (max 100 words)

Yuya Ashida received his Ph.D. degree in 2020 from the University of Tokyo under the supervision of Professor Yoshiaki Nishibayashi, focusing on the development of novel catalytic nitrogen fixation reactions. Upon finishing his Ph.D. study, he began a postdoctoral appointment in the same laboratory.

Yoshiaki Nishibayashi received his Ph.D. in 1995 from Kyoto University under the supervision of Professor Sakae Uemura. He became an assistant professor at the University of Tokyo in 1995 and moved to Kyoto University in 2000. In 2005, he became an associate professor at the University of Tokyo as PI. Since 2016, he has been a full professor at the University of Tokyo. His current research interests are organic and organometallic chemistry.